

PALAEOENVIRONMENTAL STUDY AND SMALL SCALE CORRELATIONS USING FACIES ANALYSIS AND MAGNETIC SUSCEPTIBILITY OF THE MID-EMSIAN (HIMMELBAACH QUARRY, LUXEMBOURG)

Jonathan MICHEL¹, Frédéric BOULVAIN¹, Simon PHILIPPO² & Anne-Christine DA SILVA¹

(8 figures)

¹Université de Liège, Pétrologie sédimentaire, Allée du 6 Août, B20, Sart-Tilman, B-4000 Liège, e-mail : jmichel@student.ulg.ac.be

²Musée National d'Histoire Naturelle du Luxembourg, 25 rue Münster, Luxembourg, L-2160.

ABSTRACT. The Himmelbaach quarry is located in the Wiltz Synclinorium in Luxembourg. The rocks outcropping in this quarry correspond to the mid-Emsian Clervaux Shales Formation. Three different facies have been identified in the quarry. An argillaceous sandstone facies with oblique stratifications, cross-stratifications, herring-bones and erosive bases represent the first facies; the second facies is characterized by lenticular- (with connected lenses) to wavy-bedded sandy argillites, argillaceous sandstones and quartz arenites. The last facies corresponds to a quartz arenite with oblique stratification, planar laminations and mud drapes. The base of this facies shows flaser bedding and sigmoidally curved bed surfaces. The palaeoenvironmental study of this area is rather difficult because of the structural deformation and lateral variation of the facies. Due to this deformation, six partial sections (4a to 4f) were sampled here. In order to reconstruct a reliable vertical and lateral succession of the depositional setting, facies analysis and magnetic susceptibility were used. Magnetic susceptibility (MS) is generally applied as a tool for correlation in a deepwater carbonated environment. In this paper we used the MS technique successfully in a siliciclastic proximal setting. Analysis of MS curves as well as the recognition of three marker beds ((1) the last bed of argillaceous sandstones in Facies 1; (2) a thin horizon of carbonated sandstone within Facies 2; (3) the first appearance of the characteristics massive quartzitic beds in Facies 3) allowed the correlation of sections 4a, 4b and 4c. These correlations helped us to reconstruct a vertical and lateral succession of facies, which ultimately led to the recognition of a tide-dominated marginal-marine depositional model composed respectively of tidal channels (Facies 1), a tidal flat (Facies 2) and a tidal sand ridge (Facies 3). This example also shows the usefulness of magnetic susceptibility for small scale correlation, even in a proximal environment such as a marginal-marine setting.

KEYWORDS: Emsian, Luxembourg, magnetic susceptibility, tide-dominated environment.

1. Introduction

The Lower Devonian is a particular period of interest because it is characterized by the first transgression of the Rheic Ocean, after the Caledonian orogeny, on the coasts of the Old Red Continent (Bultynck & Dejonghe, 2001). These transgressions are marked by siliciclastic deposits in the Ardenne Basin (Fig. 1A). From the Lochkovian to the Upper Emsian, the basin underwent various stages of development, which merit detailed study. One of these episodes is recorded in the Neufchâteau-Wiltz-Eifel Synclinorium (southern part of this basin, see Fig. 1A). Lower Devonian rocks in the Neufchâteau-Wiltz-Eifel Synclinorium mainly consist of up to 4000 m of quartzitic sandstones, siltstones and silty-sandy shales.

Reliable reconstructions of palaeoenvironmental conditions are difficult due to limited outcrop exposure, the scattered occurrence of fossiliferous horizons and strong tectonic deformations. All these features also lead to significant difficulties in distinguishing between marine, brackish and terrestrial settings (Wehrmann et al., 2005). In this paper, we intend to bypass these difficulties by

applying a set of new techniques for this area and to propose a palaeoenvironmental model. The Himmelbaach quarry was selected carefully to offer an interesting stratigraphical interval as well as the best exposure conditions. However, as in the whole area, the Variscan orogeny has strongly affected the quarry. Only short successions separated by faults can be studied. This active quarry is located at 1 km to the SE of Erpeldange (9648, Diekirch, Luxembourg). The GPS coordinates are N 49° 58.448'; E 05° 57.655'.

The main goals of this study are: (1) to identify different depositional environments by facies analysis. This facies analysis is also used to correlate the several short sections sampled by the identification of marker beds; (2) to refine these correlations using bulk magnetic susceptibility analysis. The combination of the two techniques allows us to reconstruct a reliable vertical succession of the depositional environment in the quarry. Notably, MS is applied here on shallow siliciclastic sediments, which is relatively uncommon for this technique (see also Debacker et al., this volume).

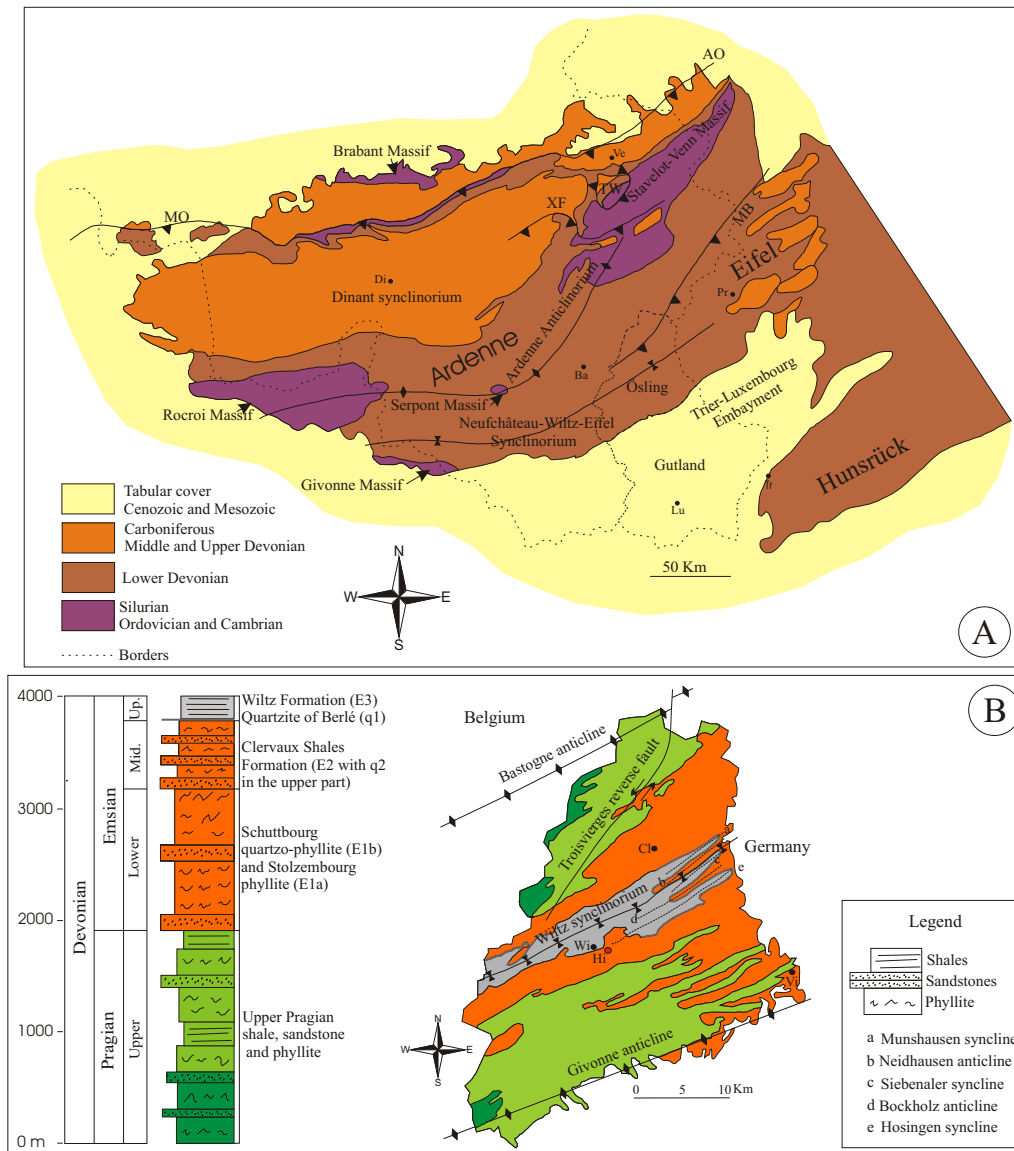


Figure 1. Geology and location of the study area. (A) Simplified geological map of the Ardennes and the Western Rheinische Schiefergebirge (modified after Bultynck & Dejonghe, 2001; Désiré-Marchand, 1985; Kenis & Sintubin, 2007; Whermann et al., 2005). Abbreviations: AO, Aachen Overthrust; Ba, Bastogne; Di, Dinant; Lu, Luxembourg; MB, Malsbenden Fault; MO, Midi Overthrust; Pr, Prüm; Tr, Trier; TW, Theux Window; Ve, Vervier; XF, Xhoris Fault. (B) Geological map of Ösling. Abbreviations: Cl, Clervaux; Hi, Himmelbaach Quarry; Vi, Vianden; Wi, Wiltz.

1.1. Geological context

Luxembourg is divided into two main morphostructural units: the “Ösling area” (the northern third of the country), belongs to the Rhenohercynian Fold and Thrust Belt while the “Gutland area”, belongs to the north eastern margins of the Paris Basin (Désiré-Marchand, 1985). The Ösling area lies between the Rocroi and Serpont Massifs in the West, the Eifel region in the East and the Stavelot Massif in the North. The Gutland area is part of the Mesozoic “Trier-Luxembourg Embayment”, situated between the Ardennes-Eifel and the Hunsrück areas (Dittrich, 1988) (Fig. 1B).

The Ösling area is composed of a succession of synclines and anticlines forming the Wiltz Synclinorium (Luxembourgish part of the Neufchâteau-Wiltz-Eifel Synclinorium). The outcrops of this area date from the Upper Pragian to the Upper Emsian (see Fig. 1B). The Upper Pragian is characterized by the alternation of blue to grey phyllites, quartzophyllites and sandstone. The Lower Emsian is represented by Stolzenbourg phyllites (E1a) and by Schuttbourg phyllites and quartzophyllites

(E1b). The total thickness of the Upper Pragian and Lower Emsian formations is 3200 m. The mid-Emsian is characterized by a 600 m-thick succession of variegated shales and sandstones called the Clervaux Shales Formation (E2). Intercalations of beds of quartzite are rare in the lower part of this formation but become common in the upper part. Faber (1982) named the quartzite of the upper part of this formation “Vorläufer-Quartzit” (q2). The Upper Emsian begins with the 15 m-thick Quartzite of Berlé (q1) and is followed by a 200 m-thick unit belonging to the Wiltz Formation (E3) (Fig. 2), characterized by grey shales with carbonated nodules. Because of a lack of precise biostratigraphical framework, all these units have a greater lithological value than a stratigraphical value. Nevertheless, Kräusel & Weyland (1930), Lippert (1939) and Solle (1937) have studied the faunistical assemblage of the Ösling area. They concluded that the Stolzenbourg and Schuttbourg units are dated as being Lower Emsian; the Clervaux Shales Formation is more mid-Emsian and the Quartzite of Berlé and the Wiltz Formation are Upper Emsian units. In the Ösling area the

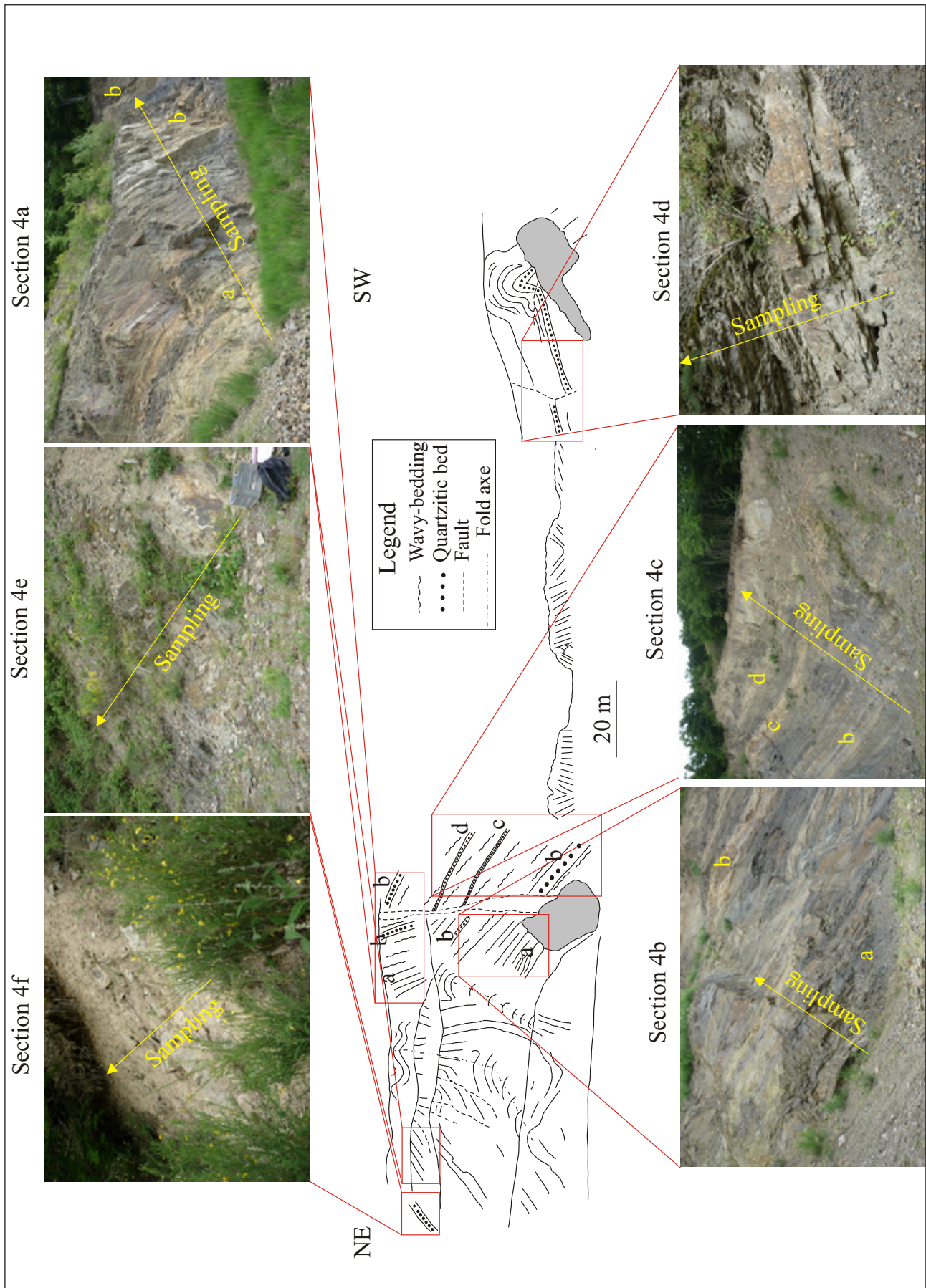


Figure 2. Locations of the measured sections in the Himmelbaach Quarry.

upper part of the Upper Emsian, represented by the upper part of the Wiltz Formation, the Wetteldorf and the Heisdorf units, has been eroded (Lucius, 1950; Muller, 1980).

The Himmelbaach quarry is located in the centre of the Wiltz Synclinorium (see Fig. 1B). Some 40 m from the top of the 600 m-thick Clervaux Shales Formation is exposed in this quarry. This comprises the “Vorläufer-Quartzit”. The quarry is divided into two parts (see Fig. 2): a north eastern part and a south western part, 70 m ahead. The north eastern part is characterized by an anticline. Sections 4a (18 m-thick), 4b (10 m-thick) and 4c (28 m-thick) were sampled in the eastern part of this anticline. Sections 4e (5 m-thick) and 4f (1 m-thick) belong to the western part of the anticline. Section 4d (4 m-thick) is located in the south western part of the quarry.

1.2. Methods

Due to structural deformation (Fig. 2), six sections were sampled in order to reconstruct a vertical sedimentological sequence of the quarry. The bed by bed technique was applied to the sampling of these sections, taking into account any lithological changes. Where the beds were more than 1 m thick, two samples were collected (one at the base and one at the top of the beds). This was the case except for the top 10 m of the 4c section, which could not be sampled with this precision due to difficulty in accessing this part. It is for this reason that the MS curve for this part of the section has not been drawn. 219 samples were collected and analysed.

The samples were studied in thin-sections to complete the field observations and to allow the elaboration of a sedimentological interpretation. Classification of the rocks was based on Blatt & Tracy (1997), Mount (1985), Lundegard & Samuels (1980) and Williams et al. (1982). Visual sorting estimation was based on Longiaru (1987) and Pettijohn et al. (1972) and visual percentage estimation was based on Baccelle & Bosellini (1965). The model proposed in the discussion section is based on Bonnot-Courtois et al. (2002), Carmona et al. (2009), Dalrymple & Choi (2007), Kazuaki et al. (2001), Mángano & Buatois (2004), Mc-Eachern & Bhattacharya (2004), Mc-Ilroy (2004), Reading (1996), Ta et al. (2002), Wehrmann et al. (2005) and Yang (1989).

The magnetic susceptibility value of each sample is the average of three measurements with a KLY-3 magnetic susceptibility meter (Kappabridge, Liège University). Each sample was weighed with a precision of 0.01 g. The minimum weight per sample allowed by this meter is 10 g. These measurements allow the definition of the mass-calibrated magnetic susceptibility of each sample and the construction of magnetic susceptibility curves.

Magnetic susceptibility curves are used in this paper for correlation purposes, as in Crick et al. (1997, 2001) and Ellwood et al. (1999, 2000), but at a local scale. So, even though the identification of the carriers of the MS signal is an important task, this will not be dealt with here because it would be of no use to our correlations.

Correlations are made on the basis of magnetic susceptibility peaks, and are isochronous and facies independent (e.g. Ellwood et al., 2000; Da Silva, 2004; Da Silva & Boulvain, 2002; Mabillet et al., 2008). The MS curves are described as a succession of trends (rise or decrease in MS values) separated by extreme MS values.

2. Results

2.1. Description of facies (see Fig. 3 for a synthesis of facies)

2.1.1. Facies 1: Argillaceous sandstones with erosive bases

This facies consists of decimetre- to metre-thick beds of green medium-grained argillaceous sandstones. These argillaceous sandstones are represented by 80% coarse grains (95% quartz grains and 5% feldspar grains, both ranging from 80 to 115 μm) and 20% matrix (5% quartz grains and 15% micas, both less than 30 μm). The most common sedimentary structures observed in these rocks include planar laminations, oblique and cross-stratifications and herring-bone structures (Fig. 4A, B and C). Mud clasts and erosion structures (truncated bases) are observed on the lower bed surfaces (Fig. 4D and E). Moreover, this facies shows fining-upward sequences from argillaceous siltite to silty to sandy argillites with planar lamination. This fining-upward trend is also marked by the decreasing size of quartz grains within the argillaceous sandstones. Grain size analyses of thin-sections show a good degree of sorting.

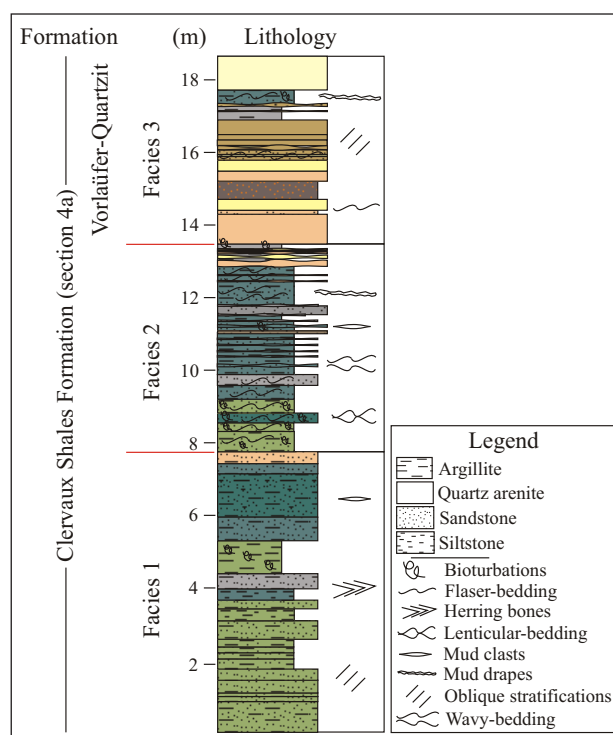


Figure 3. Facies characteristics of the Himmelbaach Quarry. The log colours correspond to the outcrop colours.



Figure 4. Facies 1. A: Argillaceous sandstone with oblique stratifications (os) (C4-01a); B: Argillaceous sandstone with through stratifications (C4-31); C: Argillaceous sandstone with planar laminations (pl) passing upward to herring bones (hb) (C4-33); D: Mud clasts in argillaceous sandstone (section 4b); E: Erosive bases in an argillaceous sandstone unit (section 4b); F: Thin section of a bimodal argillaceous sandstone (C4-01a: crossed nicols).

2.1.2. Facies 2: Lenticular- (with connected lenses) to wavy-bedded argillites, argillaceous sandstones and quartz arenites

Facies 2 consists of a millimetre- to centimetre-thick alternation of fine to medium grained green argillaceous sandstones and silty to sandy argillites. The argillaceous sandstones are represented by 70% coarse grains (95% quartz grains and 5% feldspar grains, both ranging from 60 to 110 μm) and 30% matrix (5% quartz grains and 15% micas, both less than 30 μm). The silty to sandy argillites are represented by 80% grains less than 30 μm (10% quartz grains and 90% micas) and 20% quartz grains ranging from silt to sand. The argillaceous sandstones pass upward to a medium- to coarse-grained brown to yellow quartz arenite with 97,5% coarse grains (95%

quartz grains and 5% feldspar grains, both ranging from 120 to 200 μm) and 2,5% micas less than 30 μm representing the matrix. This facies shows lenticular- (with connected lenses) to wavy-bedded structures (Fig. 5A and D). The argillaceous sandstones and quartz arenites sometimes display small asymmetrical current ripples (Fig. 5D). Moreover, mud drapes are observed at the base of these rocks (Fig. 5B). Although individual beds show lateral variation in thickness, the thickness of the bedsets is laterally stable. Evidence of bidirectional flow has been observed (Fig. 5D). A palynological study of this facies revealed a high abundance of organic matter with tracheids (Fig. 5C).

Some sandy beds are cemented by dolomite. These beds are commonly composed of well-sorted quartz grains

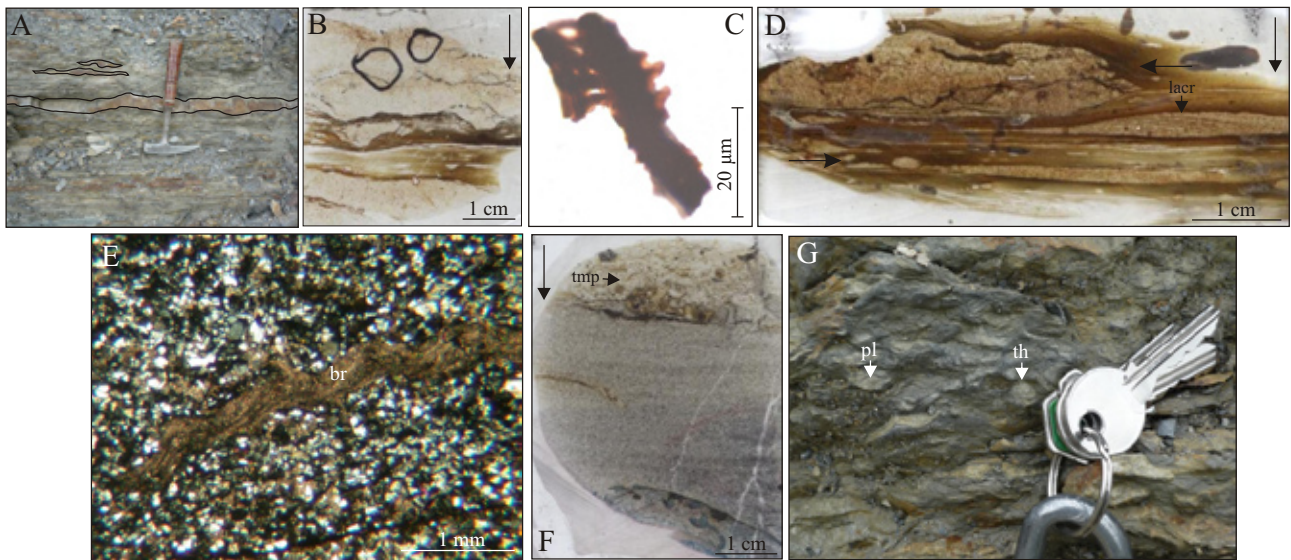


Figure 5. Facies 2. A: Lenticular-bedded to wavy-bedded quartz arenite in a pelitic unit (section 4c); B: Mud drapes in a quartz arenite (C4-77); C: Tracheid; D: Lenticular-bedded argillite with small asymmetrical current ripples in a coarse-grained laminae (lacr), arrows indicate flow directions (C4-168); E: Unbroken shell of brachiopod (br) in a well sorted carbonated sandstone (C4-50, crossed nicols); F: Carbonated sandstone with structure typical of tempestites (tmp) (C4-134b); G: Highly bioturbated shale (*Planolites* isp. (pl) and *Thalassinoides* isp. (Th), section 4c).

and dolomite crystals ranging from 80 to 120 μm . In these beds, unbroken brachiopods shells (Fig. 5E) and cricoconarids with rare entire bryozoans are observed. Locally, coarser and more poorly-sorted laminae are observed. These laminae are characterized by quartz grains and carbonated fragments of brachiopods, serpula, cricoconarid mollusca, bryozoans and crinoids, ranging

from 80 to 220 μm (Fig. 5F). Mud balls also occur in these laminae.

This facies shows a variable presence of bioturbation, ranging from intense (Fig. 5G) to nearly absent. Trace fossils are dominated by *Planolites* isp. and *Thalassinoides* isp., with rare *Palaeophycus* isp., *Spirophyton* sp. and *Diplocraterion* sp.

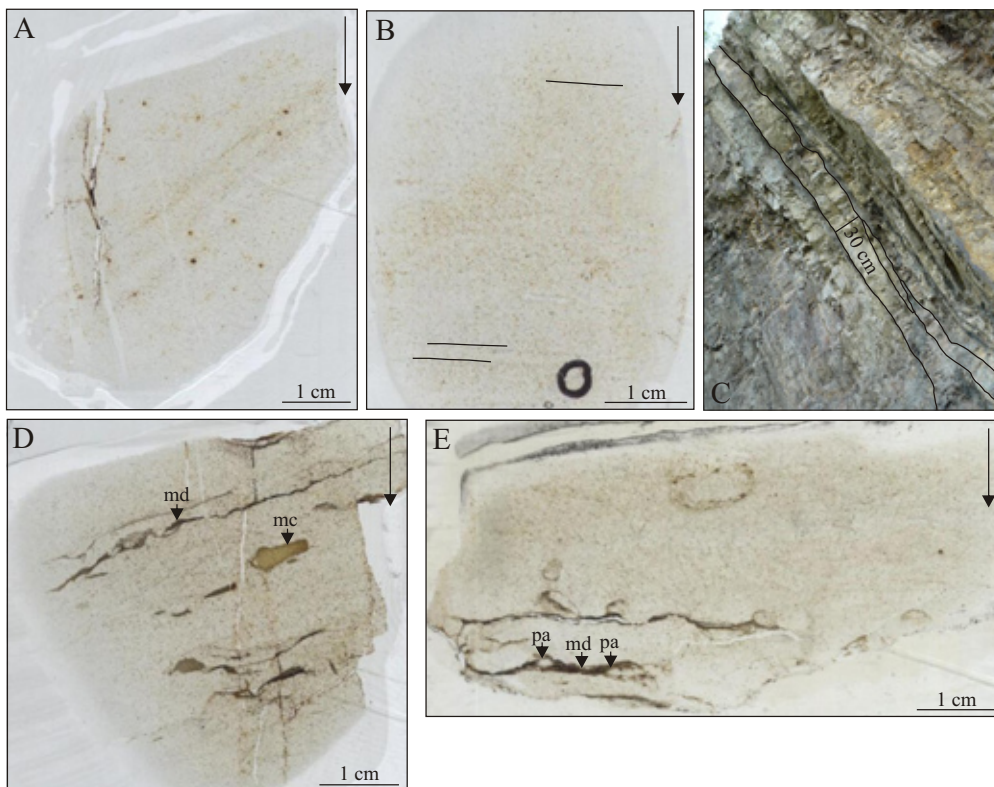


Figure 6. Facies 3. A: Quartz arenite with oblique stratifications (C4-188); B: Quartz arenite with planar laminations (C4-111); C: Channelized structure in a quartzitic unit (section 4a); D: Quartz arenite with mud drapes (md) and mud clasts (mc) (C4-95); E: Quartz arenite with bioturbated mud drapes (md) (*palaeophycus* isp. (pa)) (C4-117a).

2.1.3. Facies 3: Quartz arenites with mud drapes

This facies is represented by decimetre- to metre-thick beds of medium to coarse grained quartz arenite with oblique stratification or planar laminations (Fig. 6A and B). The quartz arenite is represented by 99% coarse grains (95% quartz grains and 5% feldspar grains, both ranging from 150 to 200 μm) and 1% micas less than 30 μm representing the matrix. Locally, argillaceous horizons or laminae were observed between these beds. Channelized structures occur (Fig. 6C) as well as beds with sigmoidal contacts. Mud drapes and mud clasts are common (Fig. 6D and E). Cross-stratifications are also present. The intensity and diversity of bioturbation is commonly low. Scarce *Thalassinoides* isp. and *Planolites* isp were identified. This facies is represented at the top of the 4a section by beds of quartz arenite. Laterally, variation appears with the intercalation of wavy-bedded silty- to sandy argillite corresponding to Facies 2 between these quartz arenites.

2.2. Description of magnetic susceptibility curves (see Fig. 7)

The values of section 4a range from $20 \times 10^{-9} \text{ m}^3/\text{kg}$ to $120 \times 10^{-9} \text{ m}^3/\text{kg}$. The highest values are observed for the lower part of the curve and range from $65 \times 10^{-9} \text{ m}^3/\text{kg}$ to $180 \times 10^{-9} \text{ m}^3/\text{kg}$. Six extreme values are observed: (a) $164.70 \times 10^{-9} \text{ m}^3/\text{kg}$, (b) $187.60 \times 10^{-9} \text{ m}^3/\text{kg}$, (c) $80.25 \times 10^{-9} \text{ m}^3/\text{kg}$, (d) $156.20 \times 10^{-9} \text{ m}^3/\text{kg}$, (e) $3.35 \times 10^{-9} \text{ m}^3/\text{kg}$ and (f) $5.11 \times 10^{-9} \text{ m}^3/\text{kg}$ (respectively from bottom to top).

For section 4b, the values range from $50 \times 10^{-9} \text{ m}^3/\text{kg}$ to $90 \times 10^{-9} \text{ m}^3/\text{kg}$. Three extreme values were recorded from bottom to top: (a) $92.69 \times 10^{-9} \text{ m}^3/\text{kg}$, (b) $94.41 \times 10^{-9} \text{ m}^3/\text{kg}$ and (c) $58.58 \times 10^{-9} \text{ m}^3/\text{kg}$.

Section 4c is characterized by values ranging from $20 \times 10^{-9} \text{ m}^3/\text{kg}$ to $100 \times 10^{-9} \text{ m}^3/\text{kg}$ and three extreme values are observed: (d) $149.50 \times 10^{-9} \text{ m}^3/\text{kg}$ (e) $6.46 \times 10^{-9} \text{ m}^3/\text{kg}$ and (f) $8.13 \times 10^{-9} \text{ m}^3/\text{kg}$ (respectively from bottom to top).

The values of sections 4d, 4e and 4f range respectively from 20×10^{-9} to $80 \times 10^{-9} \text{ m}^3/\text{kg}$, 10×10^{-9} to $100 \times 10^{-9} \text{ m}^3/\text{kg}$ and 0 to $80 \times 10^{-9} \text{ m}^3/\text{kg}$.

3. Discussion

3.1. Correlations

Facies analysis allows us to identify three marker beds (see Fig. 7). These marker beds represent limits between facies or particular horizons within these facies. The marker beds are: (1) the last argillaceous sandstone beds in the top of Facies 1 (M.b.1), which were identified and correlated in sections 4a and 4b; (2) the thin horizon of carbonated sandstone beds with accumulations of bioclasts within Facies 2 (M.b.2) (see 2.1.2.) is a good marker for correlating sections 4a and 4c; (3) the first appearance of the massive quartzitic bed (Facies 3) (M.b.3) which is observed in the top of section 4a and in the lower part of section 4c. Sections 4d, 4e and 4f are too thin to be correlated using this method.

Analysis of magnetic susceptibility curves leads to the identification of several trends and peaks (extreme values) in sections 4a, 4b and 4c. All these features allow us to make the following correlations (see Fig. 7):

In section 4b, trends 1 and 2 and peaks a, b and c from section 4a are identified. However, this section does not display peak d at the top of trend 2, suggesting that this trend is not completely represented. If we look at the peak b in section 4a and 4b, we can see that this peak occur in argillite in section 4a and in sandstone in section 4b. This may suggest that MS signal is facies independent event in a siliciclastic deposit.

For section 4c, trend 3 and peaks e, d and f are present.

The low thickness of sections 4d, 4e and 4f does not allow us to recognize any tendency or peaks on the MS curves that can be correlated with the other sections.

3.2. Facies interpretation

3.2.1. Facies 1: Argillaceous sandstones with erosive bases

The presence of oblique stratification passing upwards to planar laminations, added to the presence of cross-stratifications and herring-bones, indicates variations in flow velocity and direction (Collinson & Thompson, 1989). The presence of mud clasts, although not exclusive from tidal settings, also suggests a tidal influence (Carmona et al., 2009; Dalrymple & Choi, 2007; Wehrmann et al., 2005). The occurrence of erosive bases, oblique stratification and a fining-upward trend fits with a channelized geometry (Collinson & Thompson, 1989; Reading, 1996). All these characteristics indicate that Facies 1 represents tidal channels.

3.2.2. Facies 2: Lenticular- (with connected lenses) to wavy-bedded argillites, argillaceous sandstones and quartz arenites

The presence of lenticular and wavy-bedded structures suggests a tide-dominated environment. The coarse-grained laminae were deposited during current action periods, whereas the fine-grained laminae were deposited during calm periods (Carmona et al., 2009). The occurrence of mud drapes in the coarse-grained laminae reveals that mud material was deposited during slack water (Carmona et al., 2009). Tidal current activity is also suggested by the bidirectional pattern of the flow. A transition, in the coarse-grained laminae, from argillaceous sandstones to quartz arenite suggests an increase in the energy of the environment. The important quantity of organic matter, particularly of tracheids, points to a proximal trend in this environment. Moreover, according to Holland & Elmore (2008) and Ta et al. (2002), the presence of non-broken brachiopods shells and cricoconarids with rare entire bryozoans is due to biological activity, which is galvanized by the emergence of the environment during low tides. However, the occurrence of fragments of brachiopods, serpula, cricoconarid mollusca, bryozoans and crinoids, the poor sorting of the material, as well as the presence of mud balls, also indicate storm activity and these beds might be interpreted as tempestites.

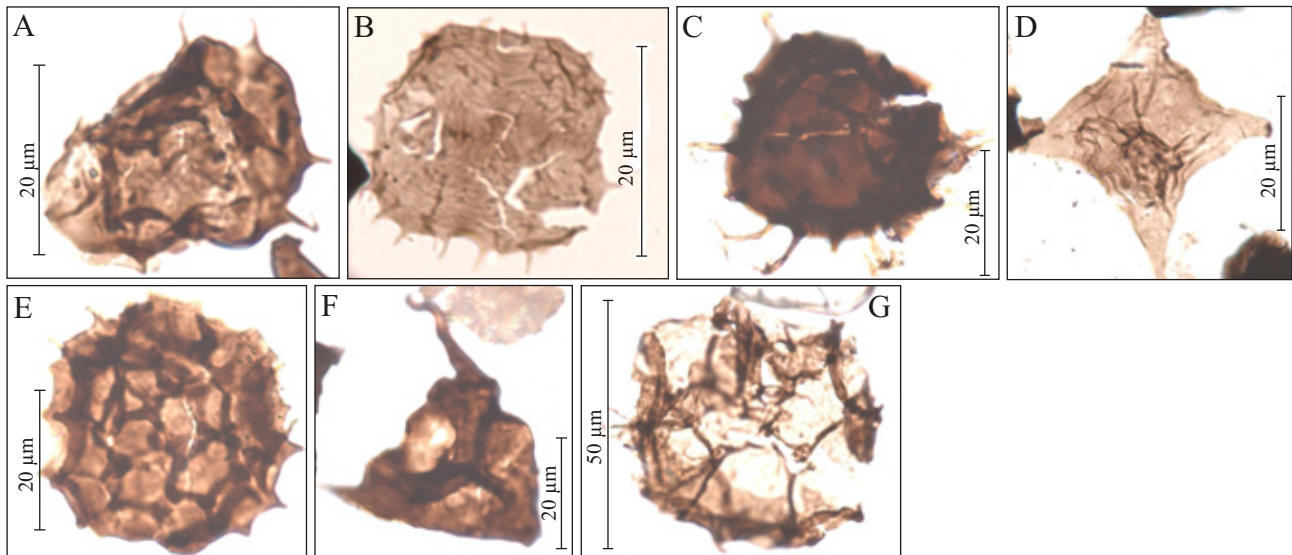


Figure 8. Clervaux Shales reworked acritarchs. A, *Acanthodiacrodictus* sp.; B, *Coryphidium* sp.; C, *Stelliferidium* sp.; D, *Striatotheca* sp.; E, *Timofeevia* sp.; F, *Veryhachium trispinosum* groupe; G, *Vulcanisphaera* sp.

Finally, variations in bioturbation intensity indicate a variable environmental stress. The poorly bioturbated units could suggest a salinity stressed environment. In this case, rises in bioturbation intensity would indicate periods of normal conditions (Carmona et al., 2009; Mc-Eachern & Bhattacharya, 2004 and Mc-Ilroy, 2004). Facies 2 is interpreted as representing a tidal flat.

3.2.3. Facies 3: Quartz arenites with mud drapes

The presence of cross-stratification combined with mud drapes indicates variations in flow velocity and direction (Willis et al., 1999), corresponding to environments with a strong tidal influence (Carmona et al., 2009). The presence of mud clasts supports this interpretation (Dalrymple & Choi, 2007; Wehrmann et al., 2005). The relatively high frequency of oblique stratifications suggests a predominant bedload transport (Collinson & Thompson, 1989; Carmona et al., 2009). The lateral intercalations of Facies 2 within this facies indicate a lenticular shape of the quartz arenite succession (Dürkoop, 1992; Faber, 1982). On the basis of facies succession (Fig. 7), this facies is considered to be deposited seaward of Facies 1 (tidal channels) and Facies 2 (tidal flat). The high percentage of quartz grain, its distal position compared to the other facies, its lenticular shape and the occurrence of tidal structures suggest that Facies 3 represents a tidal sand ridge (Kazuaki et al., 2001).

3.3. Sedimentary model

The model proposed in this paper corresponds to a marginal-marine tide-dominated environment. According to Antun (1950), the identification of *Spirophyton* sp. indicates a marine to brackish water setting corresponding to a littoral to sublittoral environment. Franke (2006) also observed these ichnofossils in the Clervaux Shales Formation and described them as a reoccupation facies fauna in a tidal flat. Indeed, he observed the presence of

both, marine and fresh water fauna in this formation. Moreover, the variation in bioturbation intensity observed in Facies 2 (see 2.1.2.) suggests stress conditions typical of marginal-marine environments. Intensively bioturbated horizons reflect normal condition whereas poorly bioturbated horizons reflect a salinity stressed condition (Carmona et al., 2009; Mc-Eachern & Bhattacharya, 2004; Mc-Ilroy, 2004).

Although tidal influence can be established on the basis of physical sedimentary structures and associated facies, identifying whether tidal facies were formed in a delta or estuary setting is not straightforward because these facies occur in both environments.

Traditionally, geomorphologists have distinguished emergent from submergent coasts on the basis of falling and rising sea levels (Johnson, 1919). Fisher et al. (1969) classified coasts according to these principles. This classification was enhanced by many authors from Galloway (1975) to Dalrymple et al. (1992). All of these authors suggested that the transformation of one type of coast into another is due to change in the nature of sedimentary supply and the fluctuation of relative sea level. According to this classification, transgressive trends are more favourable to the development of an estuary than of a deltaic setting.

Although the facies succession of the Himmelbaach quarry is transgressive, a complete palaeoenvironmental study of the Neufchâteau-Wiltz-Eifel Synclinorium is needed to document the existence of a transgressive trend throughout the basin. Nevertheless, Asselberghs (1944) in his lithological study of the Neufchâteau-Wiltz-Eifel Synclinorium, compared Belgian, Luxembourgish and German rocks. He concluded that the older succession of this Basin (Upper Pragian) represents a regressive phase in the basin history. This regression ended in the 2/3 lower part of the mid-Emsian with an emersion surface. After that began a transgression in the 1/3 upper part of the mid-

Emsian (the period of interest of this paper) continuing through the Upper Emsian. The hypothesis of the installation of an estuary in the upper part of the mid-Emsian is therefore the most probable. In this case, the facies succession of the Himmelbaach quarry represents the middle part of a tide-dominated estuary.

3.4. Possible sedimentary provenance

The palynological study of the Clervaux Shales Formation, including the Himmelbaach quarry, allows the identification of 7 cambro-ordovician reworked acritarch species: *Acanthodiacrodicus* sp., *Coryphidium* sp., *Stelliferidium* sp., *Striatotheca* sp., *Timofeevia* sp., *Veryhachium trispinosum* groupe and *Vulcanisphaera* sp. (see Fig. 8). These acritarchs were previously observed in the Brabant and Stavelot Massifs (Breuer & Vanguetaine, 2004; Vanguetaine, 1991, 2008; Vanguetaine & Servais, 2002). However, the emersion of the Stavelot Massif probably started only during the late Emsian (Colbeaux et al., 1977).

Concerning the Brabant Massif, there is no simple answer regarding the exact timing of its deformation and therefore its uplift (Debacker et al., 2005). The first hypothesis is that the deposition of the late Emsian to early Eifelian Burnot conglomerate corresponds to the first unroofing of the massif (Debacker et al., 2005; Dewaele et al., 2002; Michot et al., 1973). In this case, the Brabant Massif as a source for the mid-Emsian Clervaux Shales Formation is not an option. On the other hand, according to Steemans (1989) and other data from Debacker et al. (2005) and Dewaele et al. (2002), the emersion of the Brabant Massif would have begun in the late Silurian to early Early Devonian. So the source of the Cambro-Ordovician reworked acritarchs could be found in the Brabant Massif. Another possible source area is the Mid-German crystalline rise. To solve this question, palaeocurrent studies need to be undertaken in the Neufchâteau-Wiltz-Eifel Synclinorium. Measurement of the palaeocurrents in the Himmelbaach quarry is extremely difficult because the measurable structures occur principally on the stratification surface of displaced blocks. The oblique stratifications are not visible and not numerous enough to indicate a clear palaeocurrent direction.

4. Conclusion

This paper explores the mid-Emsian detritic formation observed in Northern Luxembourg, in the Himmelbaach quarry. The study of this formation is particularly difficult because of strong lateral variations of facies and strong deformations. In order to circumvent these problems, we used a combination of detailed sedimentological analysis (6 sections studied) and magnetic susceptibility (for correlation purposes). Detailed facies analysis led to the recognition of three facies: (1) argillaceous sandstones with erosive bases; (2) lenticular- (with connected lenses) to wavy-bedded argillites, argillaceous sandstones and quartz arenites; (3) quartz arenites with mud drapes.

Magnetic susceptibility led to the correlation of the 3 longer sections and to the proposal of a more consistent vertical and lateral facies succession. These vertical and lateral profiles, combined with the detailed sedimentology enabled us to propose a reliable palaeoenvironmental reconstruction of the area and of its evolution through the studied stratigraphic interval. Palaeoenvironments correspond to tidal channels, a tidal flat and a tidal sand ridge and represent a tide-influenced marginal-marine environment. The vertical succession of these environments allows us to identify a transgressive trend, which could possibly be a part of an estuary setting.

In conclusion, the combination of these techniques, allowed us to propose a vertical and lateral succession model of this strongly deformed marginal-marine depositional setting. We also showed that MS can be used with success in these very proximal (almost continental) settings.

5. Acknowledgments

We thank Olivier Bolle for his helpful comments in the field. We also thank Philippe Steemans and Thomas Servais for their precious participation in the palynological study and in the identification of acritarchs. We are grateful to Leona Koptikova and Timothy Debacker for their reviews. Jonathan Michel is grateful to the "Fondation Nationale de la Recherche Luxembourgeoise" for his PhD grant (TR-PHD BFR07-116). AC Da Silva acknowledges the F.N.R.S. for a position as postdoctoral researcher.

6. References

- ANTUN, P., 1950. Sur les Spirophyton de l'Emsien de l'Oesling (Grand-Duché de Luxembourg). *Annales de la Société Géologique de Belgique*, 73: 241-261.
- ASSELBERGHS, E., 1944. Emsien et Koblenzschichten en Ardenne, dans l'Oesling et dans l'Eifel. *Mémoires de l'Institut Géologique de l'Université de Louvain*, 13: 61-89.
- BACCELLE L. & BOSELLINI A., 1965. Diagrammi per la stimavisiva della composizione percentuale nelle rocce sedimentarie. *Annali della Università di Ferrara, Sezione IX, Science Geologiche e Paleontologiche*, 1: 59-62.
- BLATT H. & TRACY R.J., 1997. *Petrology; igneous, sedimentary, and metamorphic*. W. H. Freeman and Company, New York, United States.
- BONNOT-COURTOIS, C., CALINE, B., L'HOMER, A. & LE VOT, M., (eds), 2002. *La Baie du Mont-Saint-Michel et l'Estuaire de la Rance : Environnements sédimentaires, aménagements et évolution récente*. Bulletin du Centre de Recherche de Elf Exploration et Production, Mémoire 26. CNRS, EPHE, TotalFinaElf, Pau, France.
- BREUER, P. & VANGUESTAINE, M., 2004. The latest Tremadocian messaoudensis-trifidum acritarch assemblage from the upper part of the Lierneux Member (Salm Group, Stavelot Inlier, Belgium). *Review of Palaeobotany and Palynology*, 130: 41-58.

- BULTYNCK P. & DEJONGHE L. (eds), 2001. *Lithostratigraphic scale of Belgium*. *Geologica Belgica*, 4(1-2).
- CARMONA, N.B., BUATOIS, L.A., PONCE, J.J. & MÁNGANO, M.G., 2009. Ichnology and sedimentology of a tide-influenced delta, Lower Miocene Chenque Formation, Patagonia, Argentina: Trace-fossil distribution and response to environmental stresses. *Palaeogeography, Palaeoclimatology, Palaeoecology*, 273: 75-86.
- COLBEAUX, J.P., BEUGNIES, A., DUPUIS, C., ROBASZYNSKI, F. & SOMME, J., 1977. Tectonique de blocs dans le sud de la Belgique et le nord de la France. *Annales de la Société Géologique du Nord*, 97: 191-222.
- COLLINSON, J.D. & THOMPSON D.B., 1989. *Sedimentary Structures, Second edition*. Unwin Hyman, London, United Kingdom.
- CRICK, R.E., ELLWOOD, B.B., HASSANI, A.E., FEIST, R. & HLADIL J., 1997. Magneto-susceptibility event and cyclostratigraphy (MSEC) of the Eifelian-Givetian GSSP and associated boundary sequences in North Africa and Europe. *Episodes*, 20: 167-175.
- CRICK, R.E., ELLWOOD, B.B., HLADIL, J., HASSANI, A.E., HROUDA, F. & CHLUPAC, I., 2001. Magnetostratigraphy susceptibility of the Pridolian-Lochkovian (Silurian-Devonian) GSSP (Klonk, Czech Republic) and coeval sequence in Anti-Atlas Morocco. *Palaeogeography, Palaeoclimatology, Palaeoecology*, 167: 73-100.
- DA SILVA, A.-C., 2004. Sédimentologie de la plate-forme carbonatée frasnienne belge. *Thèse de doctorat, Université de Liège*, Liège, Belgium.
- DA SILVA, A.-C. & BOULVAIN F., 2002. Sedimentology, Magnetic Susceptibility and Isotopes of a Middle Frasnian Carbonate Platform: Tailfer Section, Belgium. *Facies*, 46: 89-102.
- DALRYMPLE, R.W. & CHOI, K., 2007. Morphologic and facies trends through the fluvial-marine transition in tide-dominated depositional systems: a schematic framework for environmental and sequence stratigraphic interpretation. *Earth-Science Reviews*, 81: 135-174.
- DALRYMPLE, R.W., ZAITLIN, B.A. & BOYD, R., 1992. Estuarine facies models: conceptual basis and stratigraphic implications. *Journal of Sedimentary Petrology*, 62: 1130-1146.
- DEBACKER, T.N., DEWAELE, S., SINTUBIN, M., VERNIERS, J., MUCHEZ, P. & BOVEN, A., 2005. Timing and duration of the progressive deformation of the Brabant Massif, Belgium. *Geologica Belgica*, 8: 20-34.
- DEBACKER, T.N., SINTUBIN, M. & ROBION, P., 2010. On the use of magnetic techniques for stratigraphic purposes: examples from the Lower Palaeozoic Anglo-Brabant Deformation Belt (Belgium). *Geologica Belgica*, this volume
- DESIRE-MARCHAND J., 1985. *Notice de la carte géomorphologique du grand-duché de Luxembourg*. Service Géologique du Luxembourg, Luxembourg.
- DEWAELE, S., BOVEN, A. & MUCHEZ, P., 2002. $^{40}\text{Ar}/^{39}\text{Ar}$ dating of mesothermal, orogenic mineralization in a low-angle reverse shear zone in the Lower Palaeozoic of the Anglo-Brabant fold belt, Belgium. *Transactions of the Institution of Mining and Metallurgy*, 111: B215-220.
- DITTRICH, D., 1988. Die 'Trier-Luxemburger Bucht'; Ein eigenständiger Senkungsraum im Nordosten der Pariser Beckens? *Nachrichten - Deutsche Geologische Gesellschaft*, 39: 14-15.
- DÜRKOOP, A., 1992. Geologie im Raum Wiltz (Luxemburg) unter besonderer berücksichtigung der Sedimentologie und Sedimentpetrographie der Bunten Schichten von Klerf (Unter-Ems) und des Quarzits von Berlé (Ober-Ems). *Diplomarbeit, Friedrichs-Wilhelms-Universität, Bonn, Germany*.
- ELLWOOD, B.B., CRICK, R.E. & HASSANI, A.E., 1999. The Magneto-susceptibility event and cyclostratigraphy (MSEC) method used in geological correlation of Devonian rocks from Anti-Atlas Morocco. *American Association of Petroleum Geologists Bulletin*, 83: 1119-1134.
- ELLWOOD, B.B., CRICK, R.E., HASSANI, A.E., BENOIST, S.L. & YOUNG, R.H., 2000. Magneto-susceptibility event and cyclostratigraphy method applied to marine rocks: Detrital input versus carbonate productivity. *Geology*, 28: 1135-1138.
- FABER, A., 1982. Contribution à la géologie du flanc méridional du Synclinal de Wiltz. *Mémoires de Licence, Faculté des Sciences, Université Libre de Bruxelles*, Brussels, Belgium.
- FISHER, W.L., BROWN, L.F.Jr., SCOTT, A.J. & MC GOWEN, J.H., 1969. *Delta Systems in the Exploration for Oil and Gas*. Bureau of Economic Geology, University of Texas, Austin, United States.
- FRANKE, C., 2006. Die Klerf-Schichten im Grossherzogtum Luxemburg, der Westeifel und von Burg Reuland. *Ferrantia*, 46: 42-96.
- GALLOWAY, W.E., 1975. Process framework for describing the morphologic and stratigraphic evolution of deltaic depositional systems. In Broussard, M.L. (ed.), *Deltas, Models for Exploration*. Houston Geological Society, Houston, 87-98.
- HOLLAND, K.T. & ELMORE, P.A., 2008. A review of heterogeneous sediments in coastal environments. *Earth-Science Reviews*, 89: 116-134.
- JOHNSON, D.W., (ed.), 1919. *Shore Processes and Shoreline Development*. John Wiley, New York, United States.
- KAZUAKI, H., YOSHIKI, S., QUANHONG, Z., XINRONG, C., PINXIAN, W., YOSHIO S. & CONGXIAN, L., 2001. Sedimentary facies of the tide-dominated paleo-Changjiang (Yangtze) estuary during the last transgression. *Marine Geology*, 177: 331-351.
- KENIS I. & SINTUBIN M., 2007. About boudins and mullions in the Ardenne-Eifel area (Belgium, Germany). *Geologica Belgica*, 10: 79-91.

- KRÄUSEL, R. & WEYLAND, H., 1930. Die Flora des deutschen Unterdevons. *Abhandlungen Preussisches geologisches Landesamt*, 131: 1-92.
- LIPPERT, H., 1939. Unterkoblenz-Fundpunkte im Norden und Westen der Sötenicher Mulde. *Senckenbergiana*, 19: 282-288.
- LONGIARU, S., 1987. Visual comparators for estimating the degree of sorting from plane and thin sections. *Journal of Sedimentary Petrology*, 57: 792-794.
- LUCIUS, M., 1950. *Erläuterungen zu der geologischen Spezialkarte Luxemburgs; Geologie Luxemburgs; das Oesling*. Publications du Service Géologique du Luxembourg, Luxembourg.
- LUNDEGARD, P.D. & SAMUELS, N.D., 1980. Field classification of fine-grained sedimentary rocks. *Journal of Sedimentary Petrology*, 50: 781-786.
- MABILLE, C., PAS, D., ARETZ, M., BOULVAIN, F., SCHRÖDER, S. & DA SILVA, A.-C., 2008. Deposition within the vicinity of the Mid-Eifelian High: detailed sedimentological study and magnetic susceptibility of a mixed ramp-related system from the Eifelian Lauch and Nohn formations (Devonian; Ohlesberg, Eifel, Germany). *Facies*, 54: 597-612.
- MÁNGANO, M.G. & BUATOIS, L.A., 2004. Ichnology of Carboniferous tide-influenced environments and tidal flat variability in North American Midcontinent. In McIlroy, D. (ed.), *The Application of Ichnology to Palaeoenvironmental and Stratigraphical Analysis*. Geological Society, London, 157-178.
- MC-EACHERN, J.A. & BHATTACHARYA, J.P., 2004. Ichnology of deltas; organism responses to the dynamic interplay of rivers, waves, storms and tides. *Annual Meeting Expanded Abstracts – American Association of Petroleum Geology*, 13: 89-90.
- MC-ILROY, D., 2004. Ichnofabrics and sedimentary facies of a tide-dominated delta: Jurassic Ile Formation of Kristin Field, Haltenbanken, Offshore Mid-Norway. In McIlroy, D. (ed.), *The Application of Ichnology to Palaeoenvironmental and Stratigraphical Analysis*. Geological Society, London, 237-272.
- MICHOT, P., FRANSSSEN, L. & LEDENT, D., 1973. Preliminary age measurements on metamorphic formations from the Ardenne anticline and the Brabant Massif (Belgium). *Fortschritte der Mineralogie*, 50: 107-109.
- MOUNT, J., 1985. Mixed siliciclastic and carbonate sediments: a proposed first-order textural and compositional classification. *Sedimentology*, 32: 435-442.
- MULLER, A., 1980. *Introduction à la géologie du Luxembourg*. Publications du Service Géologique du Luxembourg, Luxembourg.
- PETTIJOHN, F.J., POTTER, P.E. & SIEVER, R., 1972. *Sand and sandstone*. Springer-Verlag, New York, United States.
- READING, H.G., 1996. *Sedimentary Environments: Processes, Facies and Stratigraphy, Third edition*. Blackwell Science, Oxford, United Kingdom.
- SOLLE, G., 1937. *Geologie der mittleren Olkenbacher Mulde*. Abhandlungen der Senckenbergischen Naturforschenden Gesellschaft, Frankfurt, Deutschland.
- STEEMANS, P., 1989. Paléogéographie de l'Eodévien ardennais et des régions limitrophes. *Annales de la Société Géologique de Belgique*, 112: 103-119.
- TA, T.K.O., NGUYEN, V. L., TATEISHI, M., KOBAYASHI, I., SAITO, Y. & NAKAMURA, T., 2002. Sediment facies and Late Holocene progradation of the Mekong River Delta in Bentre Province, southern Vietnam: an example of evolution from a tide-dominated to a tide- and wave-dominated delta. *Sedimentary Geology*, 152: 313-325.
- VANGUESTAINE, M., 1991. Datation par acritarches des couches Cambro-Trémadociennes les plus profondes du sondage de Lessines (bord méridional du Massif du Brabant, Belgique). *Annales de la Société Géologique de Belgique*, 114: 213-231.
- VANGUESTAINE, M., 2008. Early and Middle Ordovician acritarchs of the Senne-Sennette river valleys (Brabant Massif, Belgium) and their stratigraphic implications. *Geologica Belgica*, 11: 3-24.
- VANGUESTAINE, M. & SERVAIS, T., 2002. Early Ordovician acritarchs of the Lierneux Member (Stavelot Inlier, Belgium): stratigraphy and palaeobiogeography. *Bulletin de la Société Géologique de France*, 173: 561-568.
- WEHRMANN, A., HERTWECK, G., BROCKE, R., JANSEN, U., KOENIGSHOF, P., PLODOWSKI, G., SCHINDLER, E., WILDE, V., BLIECK, A. & SCHULTKA, S., 2005. Palaeoenvironment of an Early Devonian land-sea transition; a case study from the southern margin of the Old Red Continent (Mosel Valley, Germany). *Palaos*, 20: 101-120.
- WILLIAMS, H., TURNER, F.J. & GILBERT, C.M., 1982. *Petrography; an introduction to the study of rocks in thin sections*. W. H. Freeman and Company, San Francisco, United States.
- WILLIS, B.J., BHATTACHARYA, J.P., GABEL, S.L. & WHITE, C.D., 1999. Architecture of a tide-influenced river delta in the Frontier Formation of central Wyoming, USA. *Sedimentology*, 46: 667-688.
- YANG, C.S., 1989. *Dynamics and sedimentary facies analysis of clastic tidal deposits*. Geologica Ultraiectina, Utrecht, Netherlands.